INTERFACE

rsif.royalsocietypublishing.org

Research

Cite this article: Taghian T, Narmoneva DA, Kogan AB. 2015 Modulation of cell function by electric field: a high-resolution analysis. *J. R. Soc. Interface* **12**: 20150153.
http://dx.doi.org/10.1098/rsif.2015.0153

Received: 19 February 2015
Accepted: 23 April 2015

Subject Areas:
biophysics

Keywords:
electrical cell stimulation, cell transmembrane potential, frequency-dependent response, surface charge, cell-substrate interaction

Author for correspondence:
A. B. Kogan
e-mail: koganab@UCMAIL.UC.EDU

Modulation of cell function by electric field: a high-resolution analysis

T. Taghian[1], D. A. Narmoneva[2] and A. B. Kogan[1]

[1]Department of Physics, University of Cincinnati, 345 Clifton Court, RM 400 Geo/Physics Building, Cincinnati, OH 45221-0011, USA
[2]Department of Biomedical, Chemical, and Environmental Engineering, University of Cincinnati, 2901 Woodside Dr., ML 0012, Cincinnati, OH 45221, USA

Regulation of cell function by a non-thermal, physiological-level electromagnetic field has potential for vascular tissue healing therapies and advancing hybrid bioelectronic technology. We have recently demonstrated that a physiological electric field (EF) applied wirelessly can regulate intracellular signalling and cell function in a frequency-dependent manner. However, the mechanism for such regulation is not well understood. Here, we present a systematic numerical study of a cell-field interaction following cell exposure to the external EF. We use a realistic experimental environment that also recapitulates the absence of a direct electric contact between the field-sourcing electrodes and the cells or the culture medium. We identify characteristic regimes and present their classification with respect to frequency, location, and the electrical properties of the model components. The results show a striking difference in the frequency dependence of EF penetration and cell response between cells suspended in an electrolyte and cells attached to a substrate. The EF structure in the cell is strongly inhomogeneous and is sensitive to the physical properties of the cell and its environment. These findings provide insight into the mechanisms for frequency-dependent cell responses to EF that regulate cell function, which may have important implications for EF-based therapies and biotechnology development.

1. Introduction

Electric fields (EFs) can regulate a variety of cell functions, including growth, adhesion, reorganization of cytoskeleton, contractility, differentiation, proliferation, activation of intracellular pathways, secretion of proteins and gene expression [1–7]. The regulatory effect of EFs has been demonstrated on different cell types such as neurons, osteoblasts, myoblasts, fibroblasts, endothelial cells, muscle cell and epithelial cells [8–14]. These effects result from manipulation of the native EF in the ionic extracellular environment and across the cell membrane [15–17]. The mechanisms behind cell–EF interactions are not yet understood, which limits development of EF-based therapies.

Cells can interact with the surrounding environment through receptors and ion channels embedded in the cell membranes, which transmit chemical, mechanical and electrical signals outside-in and inside-out the cells. Therefore, coupling of an electromagnetic field with the live cell can occur via either field interaction with charged molecules and proteins in the cell membrane that alters the flow of ions through the ion channels or rearranges the distribution of the membrane receptors, or via direct field penetration inside the cell and interaction with charged entities in the cytoplasm [18–20].

Experimental evidence suggests that one possible mechanism for the EF effects on cell function may involve an induced field in the cell membrane that may cause alterations in the transmembrane potential [19,21–25]. The transmembrane potential is established by the balance of intracellular and extracellular ionic concentration that generates the voltage difference across the cell membrane [21], and is maintained by ion channels, pumps and transporter proteins embedded in the cell membrane [26]. In response to the external EF, the

THE ROYAL SOCIETY PUBLISHING

induced field in the cell membrane can cause modulation of cell membrane potential, which in turn can increase the activity of the sodium, potassium or calcium channels and alter the enzyme activity of phosphates containing the voltage-sensor domain, as has been shown using genetic or pharmacological cell manipulations [18,27–29]. Depending on the EF parameters, the effects of EF can also include membrane electroporation in response to very high amplitude EF (10^7 mV mm^{-1}) (mathematical model is explained in [30–32]) and can be used in electrochemotherapy, drug delivery and gene therapy [33], as well as redistribution of membrane channels and receptors in response to non-oscillating EF with low, physiological amplitude (100 mV mm^{-1}) [25,34].

Theoretical models indicate the possibility of the high frequency (1–10 GHz), low-amplitude EF penetration into the cell via mechanisms other than electroporation, although the exact conditions for this effect are not well established [20]. Notably, this frequency range is well outside the range that is likely to be encountered physiologically (e.g. less than 1000 Hz in nervous system) without external stimulation. Recent experimental studies by us and others provide indirect support for this possibility by demonstrating that such fields may trigger a variety of intracellular signalling events that involve charge redistribution and ion flow, including signal propagation via Ca^{2+}, gap junctions or even protein–protein interactions [3,35–37].

In addition to the variation in EF parameters, the variability of methods of low-amplitude EF delivery to cells can also contribute to the diversity in the observed cell responses. EF can be delivered to cells by direct contact of electrodes with cells and the culture medium [38–42] or through a non-contact approach, which isolates electrodes from cells and the culture medium and capacitively couples EF to cells and the culture medium as reported by us [3] and others [43–46]. Overall, experimental results suggest that different combinations of EF intensity, frequency and/or polarization with respect to the cell, as well as methods of EF delivery, can elicit a variety of distinct cell responses, making mechanistic studies of the EF–cell interactions quite difficult.

The complexity of mechanisms for EF–cell interaction calls for a detailed understanding of the induced EF structure in cells subjected to electromagnetic field stimulation. Fricke [47] introduced an empirical equation for the potential induced in an ellipsoidal cell in suspension exposed to external EF. Schwan developed the first theoretical equation for the induced potential in a spherical cell in suspension exposed to external EF by analytical solution of the Laplace equation, where the cell is approximated by a spherical shell representing the cell membrane [48]. The model by Shawn treats the cell as a non-conducting membrane subjected to a constant and alternating external EF [49]. Kotnik *et al.* [50] extended Schwan's theory by taking into account the conductivity using constant, oscillating and pulsed EF. Other geometries—cylindrical, spheroidal and ellipsoidal—of cells suspended in the medium have been investigated later [51–54]. Several studies have modelled the cell as multiple concentric shells to determine the induced EF in the internal membranes [55,56]. The effect of surface charge and electrical properties such as membrane conductivity on the induced potential in spherical and non-spherical cell geometries has been examined [50,57]. Numeric finite-element modelling (FEM) [58–61] and transport lattice (TLM) models [62–64] and approaches based on equivalent circuits [65,66] have been used to examine complex cells of complex shapes immersed in an electrolyte. However, in most *in vivo* conditions, the cells are surrounded by and interact with the extracellular matrix, rather than being suspended in an electrolyte medium. While the cell–matrix interactions may play an important role in cell responses to the external EF, the effects of these interactions on the EF distribution within the cell compartments are not understood, and the comprehensive analyses of cellular responses, to our knowledge, have not been incorporated into the existing models.

The objective of this study, therefore, is to determine the effects of the EF frequency and extracellular environment on cell responses to the external EF. The model is based on the physiologically relevant configuration when parts of the cell membrane are in close contact with the extracellular substrate. The cell is modelled as a semi-spherical non-conducting shell separating two conducting regions, the culture medium and the cytoplasm, in direct contact with a flat dielectric substrate. To recapitulate our experimental configuration [3], the electrodes supplying the EF are isolated from the medium. The EF is therefore coupled to the cell and its environment capacitively, which eliminates electrochemical processes in the medium and reduces the electric current and associated ionic flow effects on the cell membrane. We obtain a high-resolution distribution of the induced EF in a wide frequency range (1 Hz–10 GHz) in the cell membrane, cytoplasm and extracellular medium. We then examine the sensitive dependence of the induced EF in the cell membrane and cytoplasm on cytoplasm electric properties. The results demonstrate that the field distribution exhibits physiologically important features that strongly depend on the EF frequency and differ substantially when compared with the all-electrolyte environment. The presented model and numerical method can be easily adapted to *in vivo* arrangements.

2. Material and methods

High-frequency structure simulator (HFSS, v. 14) software (ANSYS Corp, PA, USA) was used for numeric solutions of Maxwell's field equations. A variable-density adaptive mesh was generated to enable field calculations over a wide range of length scales, from nanometres for the membrane thickness to micrometres for the cytoplasm. The mesh was refined until an acceptable accuracy for the calculated EF was attained at all characteristic dimensions of the model. The large-scale mesh accuracy was tested by comparing the numeric results to the analytical solution (equation (2.1), given in the section below). The fine-scale mesh for intracell and membrane field calculations was refined to achieve a proper convergence of the path integrals of EF to zero along small closed paths. We verified that the meshes used in the simulations were sufficiently dense to produce mesh density-independent simulation output. Dimensions used in the simulation and material parameters [20,66–69] are given in table 1.

2.1. Model system

The model follows the design of our recent experimental *in vitro* studies [3]. The electrodes used to generate the EF are isolated from the medium by dielectric spacers (figure 1*a*) and modelled as infinitely conducting planes. These electrodes define simulation boundaries. The EF produced by the electrodes is oriented perpendicular to the substrate and is influenced, at the cell location, by both the potential difference applied to the

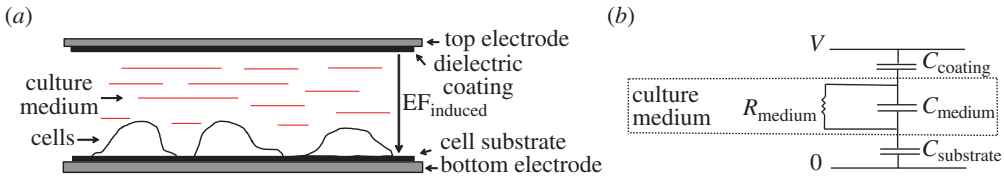

Figure 1. (*a*) Non-contact electrical stimulation of live cells. The electrodes are isolated from the culture medium by the substrate layer (bottom) and the coating layer (top). Electrodes are oriented to ensure that the resulting electric field, $EF_{induced}$, is perpendicular to the cell substrate. Cells are placed on the substrate surface which is in contact with the stimulation apparatus. (*b*) Equivalent electric circuit with no cell present. $C_{coating}$ and $C_{substrate}$ represent the capacitance of the dielectric insulating layers; C_{medium} and R_{medium} are the capacitance and resistance associated with the electrolyte (culture medium), respectively. The oscillating voltage V is applied to the top and bottom electrodes. (Online version in colour.)

Table 1. Model parameters used in the simulations.

component	parameter	value used in simulation	reference
cell membrane	thickness	5 (nm)	[67]
	relative permittivity ($\varepsilon_{membrane}$)[a]	11.3	[20]
	conductivity ($\sigma_{membrane}$)	0	[20]
cell cytoplasm	radius	5 (μm)	[66]
	relative permittivity ($\varepsilon_{cytoplasm}$)[a]	80	[68]
	conductivity ($\sigma_{cytoplasm}$)	1.5 (S m^{-1})	[69]
culture medium	relative permittivity (ε_{medium})[a]	80	[68]
	conductivity (σ_{medium})	1.5 (S m^{-1})	[69]
	height	48 (μm)	
	resistance (R_{medium})	3332 (Ω)	
	capacitance (C_{medium})	0.14 (pF)	
cell substrate	relative permittivity ($\varepsilon_{substrate}$)[a]	2.6	
	conductivity ($\sigma_{substrate}$)	0	
	thickness	1 (μm)	
	capacitance ($C_{substrate}$)	0.22 (pF)	
electrodes	electrode separation	50 (μm)	

[a]Relative permittivity: $\varepsilon_{material}/\varepsilon_{air}$.

electrodes and the substrate polarization. In the absence of cells, the system is equivalent to a one-dimensional circuit (figure 1*b*). The upper and lower capacitors represent the capacitance of the top dielectric and the substrate ($C_{substrate}$). The resistive (R_{medium}) and capacitive (C_{medium}) components of the culture medium impedance are also shown. The potential difference between the electrodes created by an external source ($V_{applied}$) creates an EF in the culture medium given by

$$EF_{induced} = \frac{\omega R_{medium} C_{substrate}}{d \times \left(4 + \left(\omega R_{medium} C_{substrate}\left(1 + 2\frac{C_{medium}}{c_{substrate}}\right)\right)^2\right)^{1/2}} V_{applied}, \tag{2.1}$$

where ω is the angular frequency of the applied field and d is the separation of the dielectric coatings. The magnitude of the EF induced in the medium, $EF_{induced}$, is plotted in figure 2 as a function of the applied field frequency. The plot is generated by Igor Pro software (WaveMetrics, OR, USA) and the values used for parameters are listed in table 1. At low EF oscillation frequency, the EF is screened from the medium by the redistribution of the ionic charges on the medium boundaries. The EF appears in the medium when the frequency becomes comparable with or larger than the characteristic inverse charging/discharging times, approximately 100 MHz for our geometry.

2.2. Modelling the cell on a substrate

The cell is modelled as a membrane-enclosed hemisphere with a realistic membrane thickness and radius attached to a substrate (extracellular matrix) and surrounded by cell-culture medium (figure 3). The cell and the substrate are non-conductive dielectrics with different dielectric permittivities (table 1). The culture medium and the cell cytoplasm are modelled as an electrolyte with ionic mobilities and concentrations that mimic those *in vivo*. The top and bottom electrodes are infinitely conducting metallic layers. Each region is homogeneous and isotropic. A 10 V potential difference is applied between the electrodes. We note that electric properties in the range of field intensities relevant to the experiments under physiological conditions are nearly independent of the field intensity; therefore, the problem is linear and describes the distribution of EF produced by an arbitrary driving voltage with an appropriate rescaling of the simulation results. We find the induced EF in the cell membrane,

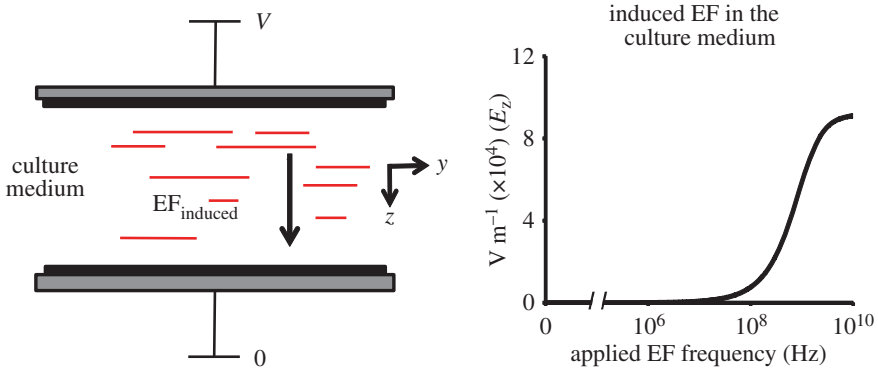

Figure 2. Induced electric field in the culture medium as a function of the applied field frequency in the non-contact model. At low frequency of the applied field, $EF_{induced}$ is excluded from the culture medium. By contrast, $EF_{induced}$ in the culture medium rises dramatically as the frequency approaches 100 MHz and reaches a constant value above 10 GHz. Electrode separation is 50 µm and $V = 10$ V. (Online version in colour.)

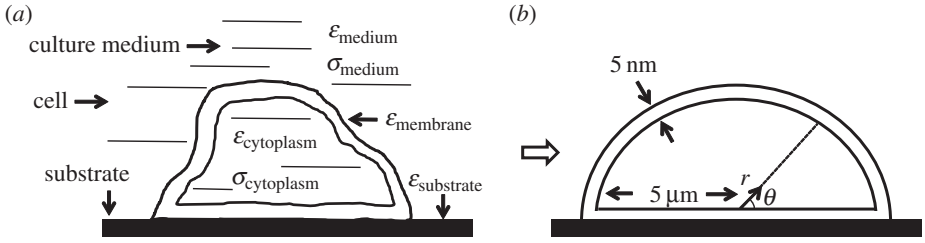

Figure 3. (*a*) Schematic of a cell attached to the substrate. (*b*) Hemispherical cell model used for simulations. Cell radius is 5 µm and membrane thickness is 5 nm (not drawn to scale). Polar coordinate system (r, θ) is used to characterize the magnitude of the induced EF in the cell membrane.

cytoplasm, extracellular medium and cell substrate by solving a full set of Maxwell's equations

$$\nabla \times E = -\frac{\partial B}{\partial t}, \quad \nabla \times H = J + \frac{\partial D}{\partial t}, \quad \nabla \cdot D = \rho \quad \text{and} \quad \nabla \cdot B = 0, \tag{2.2}$$

here, E, B, $H = B/\mu$, J and $D = \varepsilon E$ are the position- and time-dependent vectors of the EF, magnetic field, magnetic field strength, electric current density and electric displacement, μ and ε are the magnetic permeability and electric permittivity and ρ is the local density of electric charge. The induced EF is found by solving the wave equation, as follows, which is obtained by combining the first two Maxwell's equations

$$\nabla \times \left(\frac{1}{\mu_r}\nabla \times E\right) - k_0^2 \epsilon_r E = 0, \tag{2.3}$$

with

$$\mu_r = \frac{\mu}{\mu_0}, \quad \epsilon_r = \frac{\epsilon}{\epsilon_0}, \quad k_0^2 = \omega^2 \epsilon_0 \mu_0, \tag{2.4}$$

where μ_r and ϵ_r are the (generally complex-valued) relative permeability and permittivity, k_0 is the free space wavenumber and ω is the frequency of the applied EF.

The boundary conditions are fixed potentials on the two electrode boundaries, V_{top} and V_{bottom}

$$V_{bottom} - V_{top} = V \cos \omega t, \tag{2.5}$$

where V is the externally applied driving voltage and ω is the frequency of the applied field (1 Hz–10 GHz).

3. Results and discussion

3.1. Electric field distribution in the cell: frequency dependence

We first present the results of simulations at four locations along the axis of the model symmetry (figure 4): a site in the culture medium, a site inside the cytoplasm, the 'apex' and the 'substrate side' of the membrane. For all four locations, three distinct frequency regimes are identified. Region I (approx. 1 Hz–1 MHz): in agreement with the one-dimensional circuit model (figure 1), the EF is screened in the electrolyte compartments (the cytoplasm and the culture medium). Importantly, a strong field is still present in the cell membrane, both at the apex point and the substrate side. This is the central result of this work. It shows that electrodes isolated from the medium can produce EF even in free membranes, as long as a portion of the cell membrane is attached to the substrate. This is an important difference between the arrangement presented here and cells suspended in a culture medium electrolyte entirely, where no field can be produced in the membrane unless there is a penetration of the field into the electrolyte. An important implication of this finding is that even at DC voltages (as well as frequencies up to 1 MHz), manipulation of the field strength in the cell membrane can be achieved.

Region II (approx. 1 MHz–100 MHz): the penetration of the field into the cytoplasm and the culture medium develops. Both the cytoplasm and the culture medium exhibit very similar behaviour; the field in the membrane at the apex point rises and reaches values comparable with those in the substrate side of the membrane.

Region III (approx. 100 MHz–10 GHz): the penetration of the field into electrolyte is fully developed and becomes

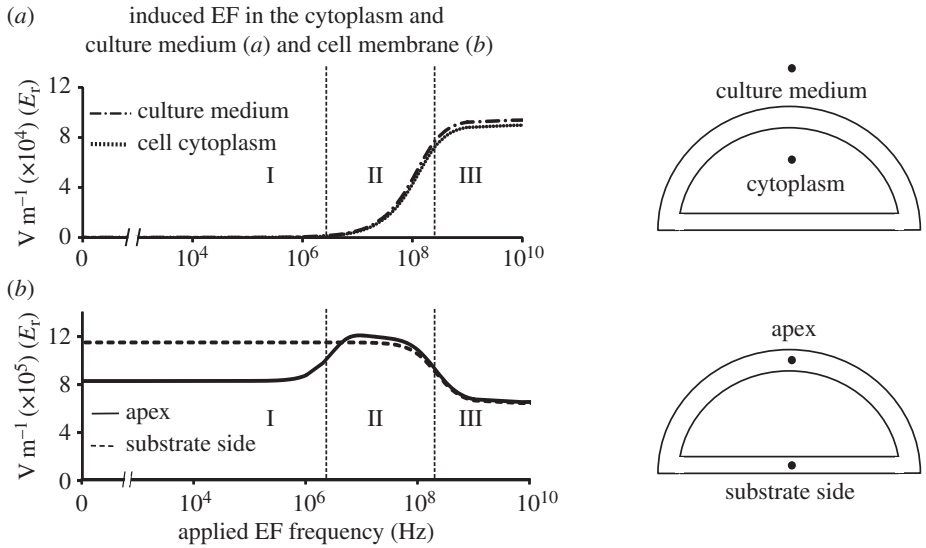

Figure 4. Frequency dependence of $EF_{induced}$ in the cell cytoplasm and the culture medium (*a*) and the cell membrane at the apex and substrate side (*b*). The response to the applied electric field can be divided into three regions. In region I, the electric field is induced in the cell membrane and is excluded from the cytoplasm and culture medium. In region II, $EF_{induced}$ in the cell membrane increases at the cell apex up to the maximum value ($E_{max} \sim 12 \times 10^5$ V m^{-1}) and starts to penetrate into the cytoplasm and culture medium, while it does not change significantly at the cell membrane facing the substrate. In region III, the magnitudes of $EF_{induced}$ at the cell apex and the substrate side both decrease and eventually reach the same plateau, while $EF_{induced}$ in the cytoplasm and culture medium both increase and also reach plateau values at high frequencies.

frequency-independent again. The fields in the apex and the substrate side of the membrane decrease slightly and reach comparable, frequency-independent values at frequencies 1 GHz and higher.

3.2. Spatial variation of electric field

Having identified the characteristic frequency domains of the problem, we turn to the spatial dependence of the induced field (figure 5). The colour plots (figure 5*a*) illustrate the EF distribution at three characteristic frequencies: 60 Hz, 10 MHz and 1 GHz. At each frequency, the EF is present in the membrane and the EF penetration to the electrolyte-filled regions is apparent as the frequency increases. In the membrane, the field is nearly homogeneous along the substrate and varies strongly through the free section of the membrane facing the medium (figure 5*b*). We also note a rapid change in the EF amplitude at points close to the cell edges.

A detailed calculation of the evolution of the angular distribution of the membrane field with frequency (figure 6) reveals two characteristic behaviours. At the locations close to the substrate ($\theta < 30^\circ$), there is a gradual decrease in the field magnitude with increasing frequency. EF distribution at the points positioned further into the free membrane section ($\theta > 50^\circ$) shows a characteristic rise to a plateau followed by the eventual reduction of the field with increasing frequency. This is similar to the 'Apex' response presented in figure 4, which corresponds to $\theta = 90^\circ$. Interestingly, the results show that the field in the substrate-facing section of the membrane close to the cell centre (line labelled 'substrate side'), far from the cell edge, is significantly stronger than the field in the low-lying points of the free membrane at all frequencies. This apparent discrepancy is a real effect that reflects the rapid change of the membrane field near the cell edge in the transition zone between the substrate-facing and the free-medium facing parts of the membrane (figure 5*a*).

3.3. Conductivity of the cytoplasm: regulation of the cell cytoplasm screening in response to electrical stimulation

Figure 7 shows the sensitivity of the induced EF at the membrane apex and substrate (figure 7*a*) and the cytoplasm (figure 7*b*) to the cytoplasm conductivity values. At the apex, a higher cytoplasm conductivity results in larger fields. In the cytoplasm itself, increasing the conductivity has the opposite effect: the higher the cytoplasm conductivity, the lower the magnitude of the induced EF. Effectively, increasing the conductivity of the cytoplasm makes the screening of the field in the cytoplasm more powerful, thus leading to increases in the in-membrane field and decreases in the cytoplasm field. As expected, the field in the membrane facing the substrate is not sensitive to the cytoplasm properties.

3.4. Substrate and culture medium properties and field penetration into the culture medium

Finally, we determine the effect of the substrate properties on field penetration (figure 8). The numeric results presented here are similar to the results obtained via the one-dimensional model (figure 2). Increasing the capacitance of the spacer layers reduces the corresponding voltage drops. As a result, the characteristic frequency at which the field begins to penetrate the medium decreases. Therefore, the high-frequency boundary of region I (figure 4) can be tuned. This observation creates an interesting opportunity for experiments that focus on intracellular effects: a measurement with a relatively low substrate capacitance at a given frequency can be used as a control as the field will be effectively screened from the cytoplasm. Increasing the substrate capacitance will introduce the field into the cytoplasm, so EF-mediated effects could be quantified. A relatively weak but notable dependence of region I width

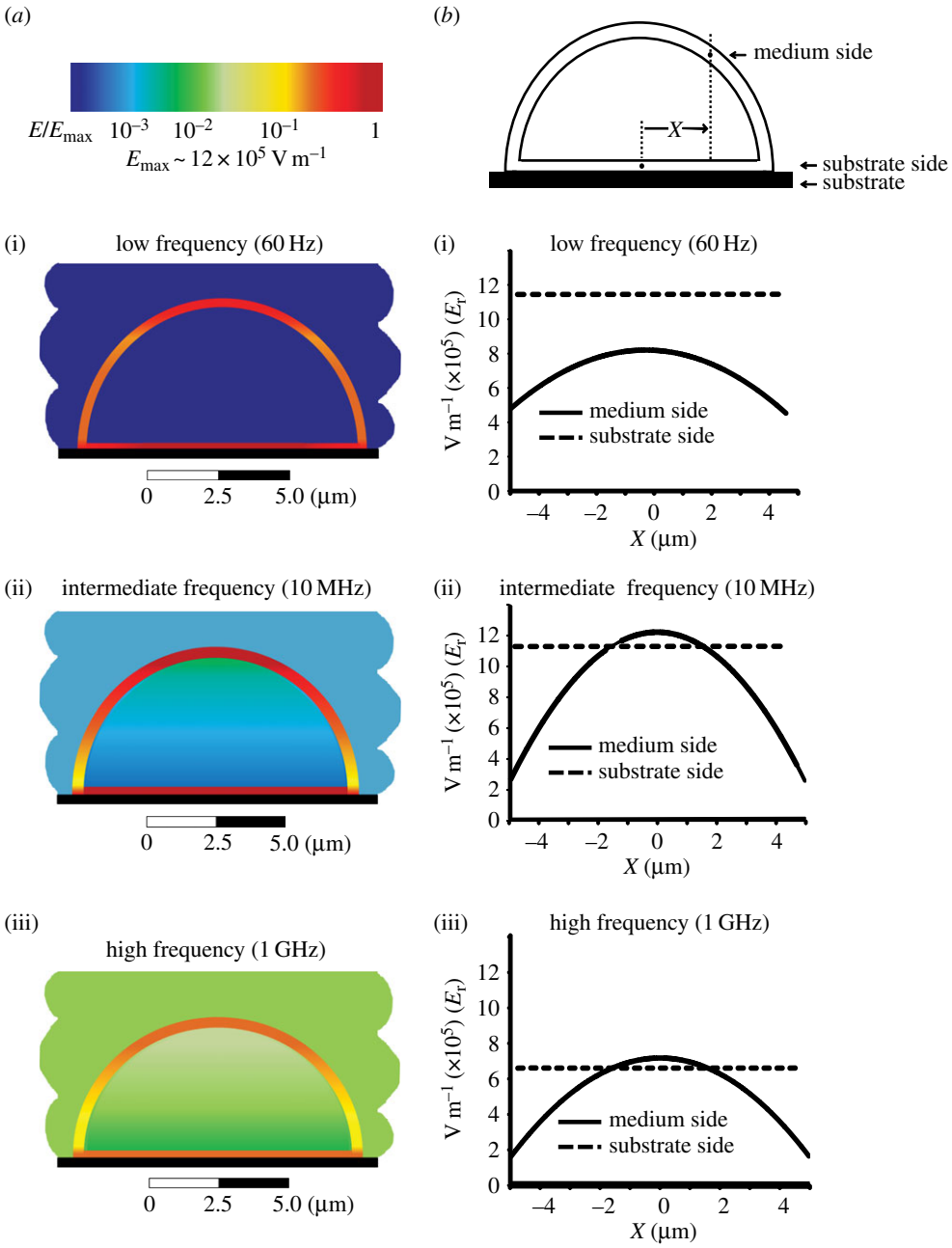

Figure 5. (*a*) Spatial distribution of the induced electric field in a single cell attached to a substrate and exposed to the external electric field that is perpendicular to the substrate. The scale applies to all colour plots, with the maximum value of $E_{max} \sim 12 \times 10^5$ V m^{-1}. At low frequency of the applied field, the induced electric field is present only in the cell membrane and is excluded from the cell cytoplasm and culture medium (i). As the frequency increases, the electric field starts penetrating into the cell cytoplasm and culture medium (ii). At high frequencies, a strong electric field is induced in all cell compartments and culture medium (iii), with the significant spatial variation in the values for $EF_{induced}$ along the cell membrane. (*b*) Distribution of $EF_{induced}$ is shown for the cell membrane facing the medium (solid line) and for the cell membrane facing the substrate (dashed line) for the same frequency ranges, demonstrating significant frequency dependence of the magnitude of the $EF_{induced}$ in the membrane at either side of the membrane.

on the culture medium and substrate properties is presented in figure 8*b*, which demonstrates that decreasing the conductivity of the medium or increasing the permittivity of the substrate results in the shift in the characteristic frequency of field penetration into the cell to the lower frequency values.

3.5. Physiological implications

Our findings demonstrate pronounced differences in cell responses to non-contact application of EF for two major configurations: cells freely suspended in the electrolyte medium and cells in direct contact with a dielectric substrate. Importantly, the latter configuration is more physiologically relevant and may describe, for example, vascular endothelial cells attached to the basement membrane, or cells within the tissues in contact with the extracellular matrix, as well as cells in contact with the implant surface. Absence of the electrolyte along parts of the membrane permits the EF to enter the cell membrane even at low frequencies and DC limit. In this regime (region I in our classification of observed field patterns with respect to frequency), this difference in cell responses between suspended and adherent configurations is the most striking: suspended cells experience no electric phenomena at low frequencies, while the cells attached to a substrate will have significant, location-dependent fields in

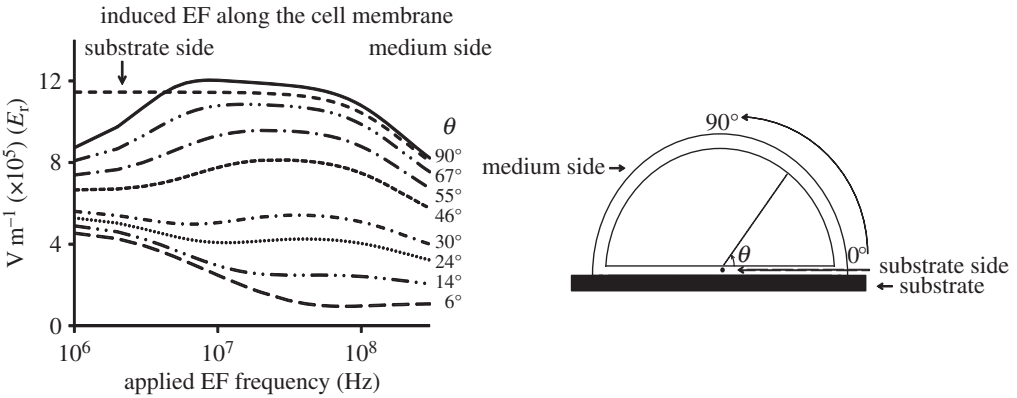

Figure 6. $EF_{induced}$ as a function of frequency of the applied field at different positions along the cell membrane. Within the 10^6–10^7 Hz range, $EF_{induced}$ increases near the apex but decreases near the substrate-facing side of the membrane.

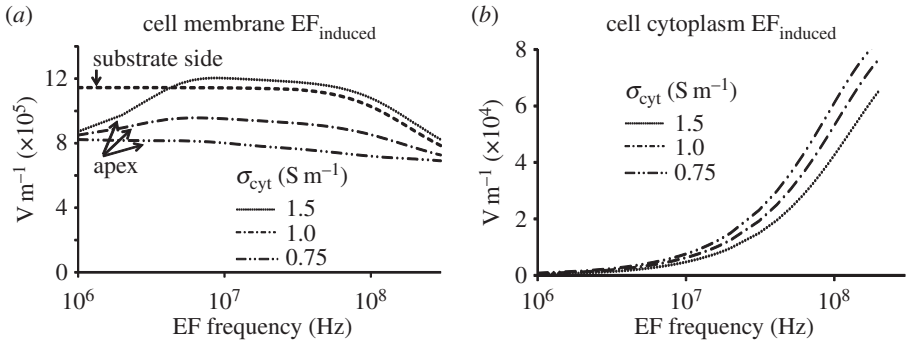

Figure 7. Effect of cytoplasm conductivity on the induced electric field in different cell compartments. (*a*) The increase in the $EF_{induced}$ at the cell apex disappears with decreasing the cytoplasmic conductivity, while $EF_{induced}$ in the membrane facing the substrate side does not depend on $\sigma_{cytoplasm}$. (*b*) Lower values of the cytoplasmic conductivity lead to a weakened cytoplasm EF screening and a shift of the EF penetration to a lower frequency.

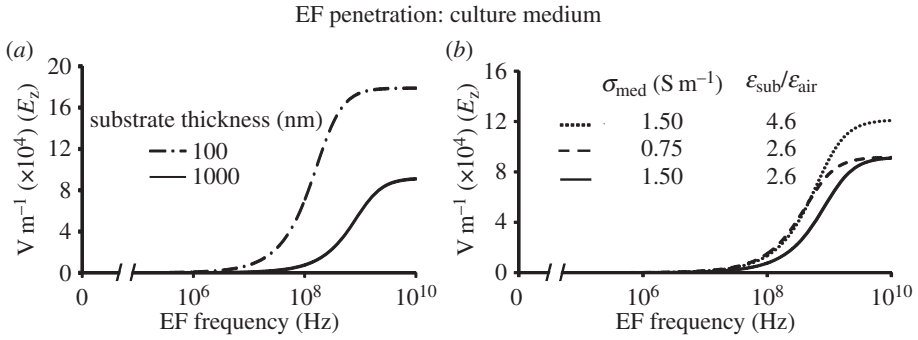

Figure 8. Effect of the geometrical and electrical parameters of the stimulation system on $EF_{induced}$ in the culture medium. (*a*) The thinner substrate allows EF penetration into the medium at lower frequencies of the applied field. (*b*) Decreasing the conductivity of the medium or increasing the permittivity of the substrate shifts the penetration frequency to lower frequencies.

the cell membrane. These fields result from the redistribution of charges in the cell-culture medium and in the cytoplasm. We have shown, therefore, that non-contact application of the EF to cells attached to non-conducting surfaces can be used to manipulate the EF in cellular membranes, which has important physiological implications. For example, several studies have reported that the alteration of the cell membrane potential can lead to the modification of the cellular structure such as redistribution of the actin cytoskeleton, changes in the localization and expression of focal adhesion proteins (e.g. vinculin) [70–74]. The induced potential evoked by the applied EF has been shown to alter the adhesive properties of cells and activation of adhesion-related proteins [4,75]. The induced membrane potential can activate signalling mechanisms (e.g. Rho/ROCK) involved in the structural alteration and increase the level of membrane proteins that regulate attachment of the cytoskeleton to the cell membrane [76–78]. The induced EF can affect voltage-gated channels embedded in the cell membrane, increase gene expression and extracellular-related proteins [43–46].

Interaction of the cell with EF changes as the field frequency increases. The EF in the membrane is retained, as an increasingly larger EF appears in the cytoplasm. This result is consistent with earlier reports that found penetration of the cytoplasm by a high-frequency EF in a free-floating configuration [20]. We show that the characteristic frequency at which the penetration of the field into the culture medium occurs can be tuned by varying the capacitance of the substrate layers and can be lowered substantially if materials with higher dielectric permittivities are used. An important

implication of this finding is that this effect can potentially be used in EF-based therapy to stimulate intracellular cell activation and desired cell responses (e.g. migration along the surface of the implant) via an appropriate combination of the implant material and the applied EF field. Indeed, in our previous studies [3], we discovered that high-frequency EF stimulation results in activation of vascular endothelial cells and angiogenic cell responses via the mechanism consistent with the model presented above. The results of the present study, therefore, may lead to the development of new approaches for vascular stents, where endothelial cell activation, proliferation and migration can be the key factor that determines success or failure of the stent [79,80].

Our results demonstrate a close relationship between cytoplasm conductivity and induced EF in the different cell compartments, which results from physiological cell homeostasis. The cytoplasmic conductivity depends on the concentration of the intracellular ions regulated by fluxes of ions into and out of the cell through ion channels in the cell membrane [81,82]. Voltage-gated ion channels can be opened in response to changes in the membrane potential to let inorganic ions diffuse down their electrochemical gradients across the cell membrane; therefore, the cytoplasm conductivity can be changed during electrical stimulation which in turn may affect the induced EF [83–85].

In this study, we have not included any dispersive, frequency-dependent terms in the dielectric properties of the materials. While small at frequencies that we have considered, these will become progressively larger as the frequency increases into tens of gigahertz and would need to be included in higher frequency calculations.

4. Conclusion

This study presents a novel model for a high-resolution microscopic analysis of the induced EF in a single cell in physiological configuration (i.e. in the electrolyte medium and attached to the extracellular substrate) exposed to the external EF. Our findings demonstrate striking differences in cell responses between cells suspended in a medium and cells attached to a dielectric substrate. We identify several characteristic regimes and present their classification with respect to frequency, location, and the electrical properties of the model components. These findings provide key information for understanding the mechanisms of cell responses to the electrical stimulation, both in the context of data interpretation from recent *in vitro* experimental results by us [3] and others [43–46], and for future therapeutic applications.

Manipulation of cells via a precisely applied EF can be used to trigger desired responses at the cell and tissue level and to restore impaired cell functions [3,6,86–92], suggesting great potential for development of safe and effective EF-based clinical treatments. To date, clinical application of EF has been reported for treatment of bone fracture, pain relief and chronic wound healing [93–97]. The majority of the stimulation devices used in clinical studies for chronic wound healing and pain relief deliver EF through generation of direct current (200–800 μA), monophasic or biphasic pulsed current with voltage ranges between 20 and 500 V [95,98–102], or using transcutaneous electrical stimulation device [103,104]. The EF current is generated between the electrodes that are placed on the skin. Although on average these therapies show a beneficial effect on wound healing, the outcomes still vary significantly, which is likely due to wide variability in the wound type, patient type, medical personnel training, electrode placement, duration of stimulation and EF parameters used for stimulation. As a result, EF-based stimulation is not currently used as a standard therapy [102,105].

Important advantages of our approach for potential EF-based wound healing therapy is in a non-contact application of EF that does not require placement of electrodes on the skin, which may improve patient comfort and treatment compliance [102,105], and may eliminate the concerns related to application of direct current EF due to pH changes in the stimulated area [98]. Our numerical model demonstrates that by non-contact application of an EF, we can induce a sufficient EF in the cell membrane and cytoplasm to manipulate protein expression and activate intracellular pathways as supported by our experimental results [3]. Such numerical modelling of EF–cell interactions is an essential and necessary part of the clinical translation process; it helps to establish therapeutic concepts and to advance approaches toward the development of non-pharmacological EF therapies [106–108], which can be applied locally and without direct contact with tissue [101,105,109–112]. Importantly, our theoretical approach can be generalized to investigate the interaction of EF with cells of an arbitrary shape. These studies, as well as an investigation of EF induced in the cell nucleus or other internal cell components and penetration of the field into tissue modelled in three-dimensional cellular arrays will be performed in the future.

Authors' contributions. Each author—T.T., D.N. and A.K.—contributed to all aspects of this research, including research design, simulations and analyses, and manuscript preparation.

Funding statement. The authors acknowledge financial support from the University of Cincinnati Physics Department (A.K. and T.T.), NSF DMR 1206784 and DMR 0804199 (A.K.), NIH 1R21 DK078814-01A1 (D.N.), the University of Cincinnati Interdisciplinary Faculty Research award (D.N. and A.K.), University of Cincinnati BCEE seed award and NSF LEAF (ADVANCE IT) (D.N.).

References

1. Radisic M, Park H, Shing H, Consi T, Schoen FJ, Langer R, Freed LE, Vunjak-Novakovic G. 2004 Functional assembly of engineered myocardium by electrical stimulation of cardiac myocytes cultured on scaffolds. *Proc. Natl Acad. Sci. USA* **101**, 18 129–18 134. (doi:10.1073/pnas.0407817101)
2. Titushkin I, Cho M. 2009 Regulation of cell cytoskeleton and membrane mechanics by electric field: role of linker proteins. *Biophys. J.* **96**, 717–728. (doi:10.1016/j.bpj.2008.09.035)
3. Sheikh AQ, Taghian T, Hemingway B, Cho H, Kogan AB, Narmoneva DA. 2013 Regulation of endothelial MAPK/ERK signalling and capillary morphogenesis by low-amplitude electric field. *J. R. Soc. Interface* **10**, 20120548. (doi:10.1098/rsif.2012.0548)
4. Zhang J, Ren R, Luo X, Fan P, Liu X, Liang S, Ma L, Yu P, Bai H. 2014 A small physiological electric field mediated responses of extravillous trophoblasts derived from HTR8/SVneo cells: involvement of activation of focal adhesion kinase signaling. *PLoS ONE.* **9**, e92252. (doi:10.1371/journal.pone.0092252)
5. Rackauskas G *et al*. 2014 Sub-threshold high frequency electrical field stimulation induces VEGF

expression in cardiomyocytes. *Cell Transplant.* **8**, 8. (doi:10.3727/096368914X682783)

6. Hernandez-Bule ML, Paino CL, Trillo MA, Ubeda A. 2014 Electric stimulation at 448 kHz promotes proliferation of human mesenchymal stem cells. *Cell Physiol. Biochem.* **34**, 1741–1755. (doi:10.1159/000366375)
7. Llucia-Valldeperas A *et al*. 2014 Physiological conditioning by electric field stimulation promotes cardiomyogenic gene expression in human cardiomyocyte progenitor cells. *Stem Cell Res. Ther.* **5**, 93. (doi:10.1186/scrt482)
8. Ahadian S, Ostrovidov S, Hosseini V, Kaji H, Ramalingam M, Bae H, Khademhosseini A. 2013 Electrical stimulation as a biomimicry tool for regulating muscle cell behavior. *Organogenesis* **9**, 87–92. (doi:10.4161/Org.25121)
9. Chiu LLY, Iyer RK, King JP, Radisic M. 2011 Biphasic electrical field stimulation aids in tissue engineering of multicell-type cardiac organoids. *Tissue Eng. A* **17**, 1465–1475. (doi:10.1089/ten.tea.2007.0244)
10. Cohen DJ, Nelson WJ, Maharbiz MM. 2014 Galvanotactic control of collective cell migration in epithelial monolayers. *Nat. Mater.* **13**, 409–417. (doi:10.1038/nmat3891)
11. Khodabukus A, Baar K. 2012 Defined electrical stimulation emphasizing excitability for the development and testing of engineered skeletal muscle. *Tissue Eng. C* **18**, 349–357. (doi:10.1089/ten.TEC.2011.0364)
12. Cameron MA, Suaning GJ, Lovell NH, Morley JW. 2013 Electrical stimulation of inner retinal neurons in wild-type and retinally degenerate (rd/rd) mice. *PLoS ONE* **8**, e68882. (doi:10.1371/journal.pone.0068882)
13. Meng S, Rouabhia M, Zhang Z. 2013 Electrical stimulation modulates osteoblast proliferation and bone protein production through heparin-bioactivated conductive scaffolds. *Bioelectromagnetics* **34**, 189–199. (doi:10.1002/Bem.21766)
14. Kobelt LJ, Wilkinson AE, McCormick AM, Willits RK, Leipzig ND. 2014 Short duration electrical stimulation to enhance neurite outgrowth and maturation of adult neural stem progenitor cells. *Ann. Biomed. Eng.* **42**, 2164–2176. (doi:10.1007/s10439-014-1058-9)
15. Taghian T, Sheikh AQ, Kogan ABDN. 2014 Harnessing electricity in biosystems—a functional tool for tissue engineering applications. *Austin J. Biomed. Eng.* **1**, 1023.
16. Levin M, Stevenson CG. 2012 Regulation of cell behavior and tissue patterning by bioelectrical signals: challenges and opportunities for biomedical engineering. *Annu. Rev. Biomed. Eng.* **14**, 295–323. (doi:10.1146/annurev-bioeng-071811-150114)
17. Vanhaesebroeck B. 2006 Charging the batteries to heal wounds through PI3 K. *Nat. Chem. Biol.* **2**, 453–455. (doi:10.1038/nchembio0906-453)
18. Funk RHW, Monsees TK. 2006 Effects of electromagnetic fields on cells: physiological and therapeutical approaches and molecular mechanisms of interaction. A review. *Cells Tissues Organs* **182**, 59–78. (doi:10.1159/000093061)
19. Zhao M, Chalmers L, Cao L, Vieira AC, Mannis M, Reid B. 2012 Electrical signaling in control of ocular cell behaviors. *Prog. Retinal Eye Res.* **31**, 65–88. (doi:10.1016/j.preteyeres.2011.10.001)
20. Foster KR. 2000 Thermal and nonthermal mechanisms of interaction of radio-frequency energy with biological systems. *IEEE Trans. Plasma Sci.* **28**, 15–23. (doi:10.1109/27.842819)
21. Sundelacruz S, Levin M, Kaplan DL. 2009 Role of membrane potential in the regulation of cell proliferation and differentiation. *Stem Cell Rev. Rep.* **5**, 231–246. (doi:10.1007/s12015-009-9080-2)
22. Tseng A, Levin M. 2013 Cracking the bioelectric code: probing endogenous ionic controls of pattern formation. *Commun. Integr. Biol.* **6**, 22595. (doi:10.4161/cib.22595)
23. Vandenberg LN, Morrie RD, Adams DS. 2011 V-ATPase-dependent ectodermal voltage and pH regionalization are required for craniofacial morphogenesis. *Dev. Dyn.* **240**, 1889–1904. (doi:10.1002/dvdy.22685)
24. McCaig CD, Rajnicek AM, Song B, Zhao M. 2005 Controlling cell behavior electrically: current views and future potential. *Physiol. Rev.* **85**, 943–978. (doi:10.1152/physrev.00020.2004)
25. Zhao M. 2009 Electrical fields in wound healing—an overriding signal that directs cell migration. *Semin. Cell. Dev. Biol.* **20**, 674–682. (doi:10.1016/j.semcdb.2008.12.009)
26. Levin M. 2013 Reprogramming cells and tissue patterning via bioelectrical pathways: molecular mechanisms and biomedical opportunities. *Wiley Interdiscip. Rev. Syst. Biol. Med.* **5**, 657–676. (doi:10.1002/wsbm.1236)
27. Grant AO. 2009 Cardiac ion channels. *Circulation* **2**, 185–194.
28. Murata Y, Okamura Y. 2007 Depolarization activates the phosphoinositide phosphatase Ci-VSP, as detected in *Xenopus* oocytes coexpressing sensors of PIP2. *J. Physiol.* **583**, 875–889. (doi:10.1113/jphysiol.2007.134775)
29. Reid B, Zhao M. 2014 The electrical response to injury: molecular mechanisms and wound healing. *Adv. Wound Care* **3**, 184–201. (doi:10.1089/wound.2013.0442)
30. Gehl J. 2003 Electroporation: theory and methods, perspectives for drug delivery, gene therapy and research. *Acta Physiol. Scand.* **177**, 437–447. (doi:10.1046/j.1365-201X.2003.01093.x)
31. Escoffre JM, Dean DS, Hubert M, Rols MP, Favard C. 2007 Membrane perturbation by an external electric field: a mechanism to permit molecular uptake. *Eur. Biophys. J.* **36**, 973–983. (doi:10.1007/s00249-007-0194-7)
32. Movahed S, Li D. 2011 Microfluidics cell electroporation. *Microfluid Nanofluid* **10**, 703–734. (doi:10.1007/s10404-010-0716-y)
33. Yarmush ML, Golberg A, Serša G, Kotnik T, Miklavčič D. 2014 Electroporation-based technologies for medicine: principles, applications, and challenges. *Annu. Rev. Biomed. Eng. Nanofluid* **10**, 295–320. (doi:10.1146/annurev-bioeng-071813-104622)
34. Zhao M, Pu J, Forrester JV, McCaig CD. 2002 Membrane lipids, EGF receptors, and intracellular signals colocalize and are polarized in epithelial cells moving directionally in a physiological electric field. *FASEB J.* **16**, 857–859. (doi:10.1096/fj.01-0811fje)
35. Rao VS, Titushkin IA, Moros EG, Pickard WF, Thatte HS, Cho MR. 2008 Nonthermal effects of radiofrequency-field exposure on calcium dynamics in stem cell-derived neuronal cells: elucidation of calcium pathways. *Radiat. Res.* **169**, 319–329. (doi:10.1667/RR1118.1)
36. Maioli M, Rinaldi S, Santaniello S, Castagna A, Pigliaru G, Gualini S, Fontani V, Ventura C. 2012 Radiofrequency energy loop primes cardiac, neuronal, and skeletal muscle differentiation in mouse embryonic stem cells: a new tool for improving tissue regeneration. *Cell Transplant.* **21**, 1225–1233. (doi:10.3727/096368911X600966)
37. Maioli M, Rinaldi S, Santaniello S, Castagna A, Pigliaru G, Gualini S, Cavallini C, Fontani V, Ventura C. 2013 Radio electric conveyed fields directly reprogram human dermal skin fibroblasts toward cardiac, neuronal, and skeletal muscle-like lineages. *Cell Transplant.* **22**, 1227–1235. (doi:10.3727/096368912X657297)
38. Song B, Gu Y, Pu J, Reid B, Zhao Z, Zhao M. 2007 Application of direct current electric fields to cells and tissues *in vitro* and modulation of wound electric field *in vivo*. *Nat. Protocols* **2**, 1479–1489. (doi:10.1038/nprot.2007.205)
39. Liu J, Zhu B, Zhang G, Wang J, Tian W, Ju G, Wei X, Song B. 2015 Electric signals regulate directional migration of ventral midbrain derived dopaminergic neural progenitor cells via Wnt/GSK3beta signaling. *Exp. Neurol.* **263**, 113–121. (doi:10.1016/j.expneurol.2014.09.014)
40. Bai H, Forrester JV, Zhao M. 2011 DC electric stimulation upregulates angiogenic factors in endothelial cells through activation of VEGF receptors. *Cytokine* **55**, 110–115. (doi:10.1016/j.cyto.2011.03.003)
41. Pullar CE, Baier BS, Kariya Y, Russell AJ, Horst BAJ, Marinkovich MP, Isseroff RR. 2006 β4 integrin and epidermal growth factor coordinately regulate electric field-mediated directional migration via Rac1. *Mol. Biol. Cell* **17**, 4925–4935. (doi:10.1091/mbc.E06-05-0433)
42. Fendyur A, Spira ME. 2012 Toward on-chip, in-cell recordings from cultured cardiomyocytes by arrays of gold mushroom-shaped microelectrodes. *Front. Neuroeng.* **5**, 21. (doi:10.3389/fneng.2012.00021)
43. Ahadian S, Ramón-Azcón J, Ostrovidov S, Camci-Unal G, Kaji H, Ino K, Shiku H, Khademhosseini A, Matsue T. 2013 A contactless electrical stimulator: application to fabricate functional skeletal muscle tissue. *Biomed. Microdevices* **15**, 109–115. (doi:10.1007/s10544-012-9692-1)
44. Hartig M, Joos U, Wiesmann HP. 2000 Capacitively coupled electric fields accelerate proliferation of osteoblast-like primary cells and increase bone extracellular matrix formation *in vitro*. *Eur. Biophys. J.* **29**, 499–506. (doi:10.1007/s002490000100)

45. Xu J, Wang W, Clark CC, Brighton CT. 2009 Signal transduction in electrically stimulated articular chondrocytes involves translocation of extracellular calcium through voltage-gated channels. *Osteoarthritis Cartilage* **17**, 397–405. (doi:10.1016/j.joca.2008.07.001)
46. Brighton CT, Wang W, Clark CC. 2008 The effect of electrical fields on gene and protein expression in human osteoarthritic cartilage explants. *J. Bone Joint Surg. A* **90**, 833–848. (doi:10.2106/JBJS.F.01437)
47. Fricke H. 1953 The electric permittivity of a dilute suspension of membrane-covered ellipsoids. *J. Appl. Phys.* **24**, 644–646. (doi:10.1063/1.1721343)
48. Schwan HP. 1957 Electrical properties of tissue and cell suspensions. *Adv. Biol. Med. Phys.* **5**, 147–209. (doi:10.1016/B978-1-4832-3111-2.50008-0)
49. Grosse C, Schwan HP. 1992 Cellular membrane potentials induced by alternating fields. *Biophys. J.* **63**, 1632–1642. (doi:10.1016/S0006-3495(92)81740-X)
50. Kotnik T, Bobanović F, Miklavčič D. 1997 Sensitivity of transmembrane voltage induced by applied electric fields—a theoretical analysis. *Bioelectrochem. Bioenerg.* **43**, 285–291. (doi:10.1016/S0302-4598(97)00023-8)
51. Gimsa J, Wachner D. 2001 Analytical description of the transmembrane voltage induced on arbitrarily oriented ellipsoidal and cylindrical cells. *Biophys. J.* **81**, 1888–1896. (doi:10.1016/S0006-3495(01)75840-7)
52. Valič B, Golzio M, Pavlin M, Schatz A, Faurie C, Gabriel B, Teissié J, Rols MP, Miklavčič D. 2003 Effect of electric field induced transmembrane potential on spheroidal cells: theory and experiment. *Eur. Biophys. J.* **32**, 519–528. (doi:10.1007/s00249-003-0296-9)
53. Maswiwat K, Wachner D, Gimsa J. 2008 Effects of cell orientation and electric field frequency on the transmembrane potential induced in ellipsoidal cells. *Bioelectrochemistry* **74**, 130–141. (doi:10.1016/j.bioelechem.2008.06.001)
54. Gimsa J, Wachner D. 2001 On the analytical description of transmembrane voltage induced on spheroidal cells with zero membrane conductance. *Eur. Biophys. J.* **30**, 463–466. (doi:10.1007/s002490100162)
55. Kotnik T, Miklavčič D. 2006 Theoretical evaluation of voltage inducement on internal membranes of biological cells exposed to electric fields. *Biophys. J.* **90**, 480–491. (doi:10.1529/biophysj.105.070771)
56. Vajrala V, Claycomb JR, Sanabria H, Miller Jr JH. 2008 Effects of oscillatory electric fields on internal membranes: an analytical model. *Biophys. J.* **94**, 2043–2052. (doi:10.1529/biophysj.107.114611)
57. Mezeme ME, Brosseau C. 2010 Time-varying electric field induced transmembrane potential of a core-shell model of biological cells. *J. Appl. Phys.* **108**, 14701. (doi:10.1063/1.3456163)
58. Meny I, Burais N, Buret F, Nicolas L. 2007 Finite-element modeling of cell exposed to harmonic and transient electric fields. *IEEE Trans. Magn.* **43**, 1773–1776. (doi:10.1109/Tmag.2007.892517)
59. Sebastián JL, Muñoz San Martín S, Sancho M, Miranda JM. 2004 Modelling the internal field distribution in human erythrocytes exposed to MW radiation. *Bioelectrochemistry* **64**, 39–45. (doi:10.1016/j.bioelechem.2004.02.003)
60. Ying W, Henriquez CS. 2007 Hybrid finite element method for describing the electrical response of biological cells to applied fields. *IEEE Trans. Biomed. Eng.* **54**, 611–620. (doi:10.1109/TBME.2006.889172)
61. Miller CE, Henriquez CS. 1988 Three-dimensional finite element solution for biopotentials: erythrocyte in an applied field. *IEEE Trans. Biomed. Eng.* **35**, 712–718. (doi:10.1109/10.7272)
62. Gowrishankar TR, Smith KC, Weaver JC. 2013 Transport-based biophysical system models of cells for quantitatively describing responses to electric fields. *Proc. IEEE* **101**, 505–517. (doi:10.1109/Jproc.2012.2200289)
63. Stewart Jr DA, Gowrishankar TR, Weaver JC. 2004 Transport lattice approach to describing cell electroporation: use of a local asymptotic model. *IEEE Trans. Plasma Sci.* **32**, 1696–1708. (doi:10.1109/TPS.2004.832639)
64. Gowrishankar TR, Weaver JC. 2003 An approach to electrical modeling of single and multiple cells. *Proc. Natl Acad. Sci. USA* **100**, 3203–3208. (doi:10.1073/pnas.0636434100)
65. Ramos A, Raizer A, Marques JLB. 2003 A new computational approach for electrical analysis of biological tissues. *Bioelectrochemistry* **59**, 73–84. (doi:10.1016/S1567-5394(03)00004-5)
66. Schoenbach KH, Joshi RP, Kolb JF, Chen N, Stacey M, Blackmore PF, Buescher ES, Beebe SJ. 2004 Ultrashort electrical pulses open a new gateway into biological cells. *Proc. IEEE* **92**, 1122–1136. (doi:10.1109/JPROC.2004.829009)
67. Kotnik T, Miklavčič D, Slivnik T. 1998 Time course of transmembrane voltage induced by time-varying electric fields—a method for theoretical analysis and its application. *Bioelectrochem. Bioenergetics* **45**, 3–16. (doi:10.1016/S0302-4598(97)00093-7)
68. Fear EC, Stuchly MA. 1998 Modeling assemblies of biological cells exposed to electric fields. *IEEE Trans. Biomed. Eng.* **45**, 1259–1271. (doi:10.1109/10.720204)
69. Zhadobov M, Augustine R, Sauleau R, Alekseev S, Di Paola A, Le Quement C, Mahamoud YS, Le Drean Y. 2011 Complex permittivity of representative biological solutions in the 2–67 GHz range. *Bioelectromagnetics* **19**, 20713. (doi:10.1002/bem.20713)
70. Nin V, Hernández JA, Chifflet S. 2009 Hyperpolarization of the plasma membrane potential provokes reorganization of the actin cytoskeleton and increases the stability of adherens junctions in bovine corneal endothelial cells in culture. *Cell Motil. Cytoskeleton* **66**, 1087–1099. (doi:10.1002/cm.20416)
71. Chifflet S, Hernández JA, Grasso S, Cirillo A. 2003 Nonspecific depolarization of the plasma membrane potential induces cytoskeletal modifications of bovine corneal endothelial cells in culture. *Exp. Cell Res.* **282**, 1–13. (doi:10.1006/excr.2002.5664)
72. Vernon-Wilson EF, Auradé F, Tian L, Rowe ICM, Shipston MJ, Savill J, Brown SB. 2007 CD31 delays phagocyte membrane repolarization to promote efficient binding of apoptotic cells. *J. Leukocyte Biol.* **82**, 1278–1288. (doi:10.1189/jlb.0507283)
73. Siciliano JC, Toutant M, Derkinderen P, Sasaki T, Girault JA. 1996 Differential regulation of proline-rich tyrosine kinase 2/cell adhesion kinase β (PYK2/CAKβ) and pp125(FAK) by glutamate and depolarization in rat hippocampus. *J. Biol. Chem.* **271**, 28 942–28 946. (doi:10.1074/jbc.271.46.28942)
74. Krötz F, Riexinger T, Buerkle MA, Nithipatikom K, Gloe T, Sohn HY, Campbell WB, Pohl U. 2004 Membrane potential-dependent inhibition of platelet adhesion to endothelial cells by expoxyeicosatrienoic acids. *Arteriosclerosis, Thrombosis Vasc. Biol.* **24**, 595–600. (doi:10.1161/01.ATV.0000116219.09040.8c)
75. Song G, Qin J, Yao C, Ju Y. 2008 Effect of steep pulsed electric field on proliferation, viscoelasticity and adhesion of human hepatoma SMMC-7721 cells. *Anticancer Res.* **28**, 2245–2251.
76. Waheed F, Speight P, Kawai G, Dan Q, Kapus A, Szászi K. 2010 Extracellular signal-regulated kinase and GEF-H1 mediate depolarization-induced Rho activation and paracellular permeability increase. *Am. J. Physiol.* **298**, C1376. (doi:10.1152/ajpcell.00408.2009)
77. Szaszi K, Sirokmany G, Di Ciano-Oliveira C, Rotstein OD, Kapus A. 2005 Depolarization induces Rho–Rho kinase-mediated myosin light chain phosphorylation in kidney tubular cells. *Am. J. Physiol. Cell Physiol.* **289**, 27. (doi:10.1152/ajpcell.00481.2004)
78. Zhang X, Chen X, Jia C, Geng X, Du X, Zhang H. 2010 Depolarization increases phosphatidylinositol (PI) 4,5-bisphosphate level and KCNQ currents through PI 4-kinase mechanisms. *J. Biol. Chem.* **285**, 9402–9409. (doi:10.1074/jbc.M109.068205)
79. Kawajiri H, Mizuno T, Moriwaki T, Iwai R, Ishibashi-Ueda H, Yamanami M, Kanda K, Yaku H, Nakayama Y. 2014 Implantation study of a tissue-engineered self-expanding aortic stent graft (bio stent graft) in a beagle model. *J. Artif. Organs* **18**, 48–54. (doi:10.1007/s10047-014-0796-7)
80. Jeong W, Han MH, Rhee K. 2014 The hemodynamic alterations induced by the vascular angular deformation in stent-assisted coiling of bifurcation aneurysms. *Comput. Biol. Med.* **53**, 1–8. (doi:10.1016/j.compbiomed.2014.07.006)
81. Duncan L, Shelmerdine H, Hughes MP, Coley HM, Hübner Y, Labeed FH. 2008 Dielectrophoretic analysis of changes in cytoplasmic ion levels due to ion channel blocker action reveals underlying differences between drug-sensitive and multidrug-resistant leukaemic cells. *Phys. Med. Biol.* **53**, N1–N7. (doi:10.1088/0031-9155/53/2/N01)
82. Hübner Y, Hoettges KF, Kass GEN, Ogin SL, Hughes MP. 2005 Parallel measurements of drug actions on erythrocytes by dielectrophoresis, using a three-dimensional electrode design. *IEEE Proc. Nanobiotechnol.* **152**, 150–154. (doi:10.1049/ip-nbt:20050011)

83. Fowler PW, Sansom MSP. 2013 The pore of voltage-gated potassium ion channels is strained when closed. *Nat. Commun.* **4**, 1872. (doi:10.1038/Ncomms2858)
84. Catterall WA. 2011 Voltage-gated calcium channels. *Cold Spring Harb. Perspect. Biol.* **3**, 1–23. (doi:10.1101/cshperspect.a003947)
85. Kis-Toth K *et al*. 2011 Voltage-gated sodium channel Nav1.7 maintains the membrane potential and regulates the activation and chemokine-induced migration of a monocyte-derived dendritic cell subset. *J. Immunol.* **187**, 1273–1280. (doi:10.4049/jimmunol.1003345)
86. Liu Q, Song B. 2014 Electric field regulated signaling pathways. *Int. J. Biochem. Cell Biol.* **55**, 264–268. (doi:10.1016/j.biocel.2014.09.014)
87. Arjunan KP, Friedman G, Fridman A, Clyne AM. 2012 Non-thermal dielectric barrier discharge plasma induces angiogenesis through reactive oxygen species. *J. R. Soc. Interface* **9**, 147–157. (doi:10.1098/rsif.2011.0220)
88. Sundelacruz S, Li C, Choi YJ, Levin M, Kaplan DL. 2013 Bioelectric modulation of wound healing in a 3D *in vitro* model of tissue-engineered bone. *Biomaterials* **34**, 6695–6705. (doi:10.1016/j.biomaterials.2013.05.040)
89. Seeliger C, Falldorf K, Sachtleben J, van Griensven M. 2014 Low-frequency pulsed electromagnetic fields significantly improve time of closure and proliferation of human tendon fibroblasts. *Eur. J. Med. Res.* **19**, 19–37. (doi:10.1186/2047-783x-19-37)
90. Callaghan MJ, Chang EI, Seiser N, Aarabi S, Ghali S, Kinnucan ER, Simon BJ, Gurtner GC. 2008 Pulsed electromagnetic fields accelerate normal and diabetic wound healing by increasing endogenous FGF-2 release. *Plast. Reconstr. Surg.* **121**, 130–141. (doi:10.1097/01.prs.0000293761.27219.84)
91. Athanasiou A, Karkambounas S, Batistatou A, Lykoudis E, Katsaraki A, Kartsiouni T, Papalois A, Evangelou A. 2007 The effect of pulsed electromagnetic fields on secondary skin wound healing: an experimental study. *Bioelectromagnetics* **28**, 362–368. (doi:10.1002/bem.20303)
92. Goudarzi I, Hajizadeh S, Salmani ME, Abrari K. 2010 Pulsed electromagnetic fields accelerate wound healing in the skin of diabetic rats. *Bioelectromagnetics* **31**, 318–323. (doi:10.1002/bem.20567)
93. Goldstein C, Sprague S, Petrisor BA. 2010 Electrical stimulation for fracture healing: current evidence. *J. Orthop. Trauma* **24**, S62–SS5. (doi:10.1097/BOT.0b013e3181cdde1b)
94. Liebano RE, Rakel B, Vance CGT, Walsh DM, Sluka KA. 2011 An investigation of the development of analgesic tolerance to TENS in humans. *Pain* **152**, 335–342. (doi:10.1016/j.pain.2010.10.040)
95. Ud-Din S, Bayat A. 2014 Electrical stimulation and cutaneous wound healing: a review of clinical evidence. *Healthcare* **2**, 445–467. (doi:10.3390/healthcare2040445)
96. Kloth LC. 2005 Electrical stimulation for wound healing: a review of evidence from *in vitro* studies, animal experiments, and clinical trials. *Int. J. Low. Extrem. Wounds* **4**, 23–44. (doi:10.1177/1534734605275733)
97. Franek A, Kostur R, Polak A, Taradaj J, Szlachta Z, Blaszczak E, Dolibog P, Koczy B, Kucio C. 2012 Using high-voltage electrical stimulation in the treatment of recalcitrant pressure ulcers: results of a randomized, controlled clinical study. *Ostomy Wound Manag.* **58**, 30–44.
98. Kloth LC. 2014 Electrical stimulation technologies for wound healing. *Adv. Wound Care* **3**, 81–90. (doi:10.1089/wound.2013.0459)
99. Lawson D, Petrofsky JS. 2007 A randomized control study on the effect of biphasic electrical stimulation in a warm room on skin blood flow and healing rates in chronic wounds of patients with and without diabetes. *Med. Sci. Monit.* **13**, CR258–CR263.
100. Baker LL, Chambers R, Demuth SK, Villar F. 1997 Effects of electrical stimulation on wound healing in patients with diabetic ulcers. *Diabetes Care* **20**, 405–412. (doi:10.2337/diacare.20.3.405)
101. Houghton PE, Campbell KE, Fraser CH, Harris C, Keast DH, Potter PJ, Hayes KC, Woodbury MG. 2010 Electrical stimulation therapy increases rate of healing of pressure ulcers in community-dwelling people with spinal cord injury. *Arch. Phys. Med. Rehabil.* **91**, 669–678. (doi:10.1016/j.apmr.2009.12.026)
102. Ojingwa JC, Isseroff RR. 2003 Electrical stimulation of wound healing. *J. Invest. Dermatol.* **121**, 1–12. (doi:10.1046/j.1523-1747.2003.12454.x)
103. Sebastian A, Syed F, Perry D, Balamurugan V, Colthurst J, Chaudhry IH, Bayat A. 2011 Acceleration of cutaneous healing by electrical stimulation: degenerate electrical waveform down-regulates inflammation, up-regulates angiogenesis and advances remodeling in temporal punch biopsies in a human volunteer study. *Wound Repair Regen.* **19**, 693–708. (doi:10.1111/j.1524-475X.2011.00736.x)
104. Perry D, Colthurst J, Giddings P, McGrouther DA, Morris J, Bayat A. 2010 Treatment of symptomatic abnormal skin scars with electrical stimulation. *J. Wound Care.* **19**, 447–453. (doi:10.12968/jowc.2010.19.10.79092)
105. Isseroff RR, Dahle SE. 2012 Electrical stimulation therapy and wound healing: where are we now? *Adv. Wound Care* **1**, 238–243. (doi:10.1089/wound.2011.0351)
106. Strauch B, Herman C, Dabb R, Ignarro LJ, Pilla AA. 2009 Evidence-based use of pulsed electromagnetic field therapy in clinical plastic surgery. *Aesthet. Surg. J.* **29**, 135–143. (doi:10.1016/j.asj.2009.02.001)
107. Saliev T, Mustapova Z, Kulsharova G, Bulanin D, Mikhalovsky S. 2014 Therapeutic potential of electromagnetic fields for tissue engineering and wound healing. *Cell Prolif.* **47**, 485–493. (doi:10.1111/cpr.12142)
108. Pilla AA. 2013 Nonthermal electromagnetic fields: from first messenger to therapeutic applications. *Electromagn. Biol. Med.* **32**, 123–136. (doi:10.3109/15368378.2013.776335)
109. Thakral G, LaFontaine J, Najafi B, Talal TK, Kim P, Lavery LA. 2013 Electrical stimulation to accelerate wound healing. *Diabetic Foot Ankle* **4**, 22081. (doi:10.3402/dfa.v4i0.22081)
110. Thakral G, Kim PJ, LaFontaine J, Menzies R, Najafi B, Lavery LA. 2013 Electrical stimulation as an adjunctive treatment of painful and sensory diabetic neuropathy. *J. Diabetes Sci. Technol.* **7**, 1202–1209. (doi:10.1177/193229681300700510)
111. Sun LY, Hsieh DK, Yu TC, Chiu HT, Lu SF, Luo GH, Kuo TK, Lee OK, Chiou TW. 2009 Effect of pulsed electromagnetic field on the proliferation and differentiation potential of human bone marrow mesenchymal stem cells. *Bioelectromagnetics* **30**, 251–260. (doi:10.1002/bem.20472)
112. DeSantana JM, Walsh DM, Vance C, Rakel BA, Sluka KA. 2008 Effectiveness of transcutaneous electrical nerve stimulation for treatment of hyperalgesia and pain. *Curr. Rheumatol. Rep.* **10**, 492–499. (doi:10.1007/s11926-008-0080-z)